Genetic Algorithm based L4 Identification and Psoas Segmentation

Namitha V. Benjamin[1], Robert D. Boutin[2], Abhijit J. Chaudhari[3] and Kwan-Liu Ma[1]
[1]*Department of Computer Science, University of California, Davis, CA 95616, U.S.A.*
[2]*Department of Radiology, Stanford University School of Medicine, Stanford, CA 94305, U.S.A.*
[3]*Department of Radiology, University of California Davis, Sacramento, CA 95817, U.S.A.*

Keywords: Genetic Algorithm, Psoas Muscle, L4 Identification, Region Growing, Edge Linking.

Abstract: Segmentation of the Psoas muscle is an important first step in identifying sarcopenia. Physicians use computed tomography (CT) images to track changes in muscle mass, which, in turn, act as indicators of how well a patient is responding to treatment. To measure the muscle, a radiologist segments a CT manually. This is often time consuming task and can be prone to error. In this paper we propose a novel method to segment psoas muscles from abdominal CT images. The novel approach uses imaging techniques augmented with medical anatomic knowledge. The outcome of the algorithm is two fold; first, the 4^{th} lumbar vertebra (L4) is identified from a series of CT images. Second, the psoas muscle in the identified slice, is segmented based on a genetic algorithm based edge linking method. The algorithm was applied to a series of datasets of 61 patients over the age of 65 with hip fractures, and we obtained an average match (*true positive percentage*) of 91%.

1 INTRODUCTION

"Sarcopenia" is defined as the age-related loss of skeletal muscle mass and function (Cornet et al., 2015; Santilli et al., 2014). Such a loss directly impacts muscle strength, which in turn, increases occurrence of disability in the elderly. It has become recognized as a major public health threat in our aging population, reaching an epidemic prevalence of up to 50% by the age of 80 years (Santilli et al., 2014). Recent studies show that this condition is known to occur not only with age advancement, but also as a side effect of diseases, such as cancer and cardiovascular conditions. While there is now extensive data showing sarcopenia as an important predictor of future negative outcomes for patients (e.g., physical disability, complications after surgery, death), muscle depletion is often occult clinically. The medical community now identifies it as an independent risk factor for predicting future failing human health in adults. More and more studies (Alfonso J. Cruz-Jentoft, 2019; Van Ancum, 2020) are proving that sarcopenia can be a predictive factor of post-operative morbidity as well as recovery after cancer surgeries. In an effort to standardize this process, the "European Working Group on Sarcopenia in Older People" (EWGSOP), defined mechanisms and assessment techniques to characterize sarcopenia (Alfonso J. Cruz-Jentoft, 2019). One of the techniques identified was muscle mass. This has led to several studies aiming to characterize the relationship between lean muscle mass and patient outcomes.

One of the key muscles identified for such studies is the psoas muscle. Muscle mass can be measured via either computed tomography (CT) or magnetic resonance imaging (MRI), which are diagnostic imaging techniques considered as a ground truth, by the medical community. They allow for precise determination of body composition, including non-invasive assessment of muscle mass and quality. Although these body composition data are routinely collected on 90 million CT scans and 35 million MRI scans annually in the USA, those data are not analyzed quantitatively because of two unsolved problems: 1) the massive time burden, cost, and tediousness of performing manual measurements on individual imaging examinations, and 2) the lack of normative data across large populations. If segmentation of muscle from fat and other tissues could be automated, these problems could be solved and usher in a new era of "personalized medicine", with quantitative body composition analysis performed automatically on all routine anatomical imaging exams. Diagnosis of the type and severity of sarcopenia would allow optimal prescription of treatments for muscle depletion that include

Benjamin, N., Boutin, R., Chaudhari, A. and Ma, K.
Genetic Algorithm based L4 Identification and Psoas Segmentation.
DOI: 10.5220/0010207701200127
In *Proceedings of the 14th International Joint Conference on Biomedical Engineering Systems and Technologies (BIOSTEC 2021) - Volume 2: BIOIMAGING*, pages 120-127
ISBN: 978-989-758-490-9

specific diets and exercises, as well as medications. By manually outlining muscle, the diagnosis of sarcopenia has been validated in research settings, commonly by isolating the psoas muscle at the level of the 4^{th} lumbar vertebra (L4) on CT scans (Kamiya et al., 2012; Ulf Tiede, 1996; Meesters et al., 2012). The 4^{th} lumbar vertebrae has been chosen since the psoas muscle is seen most prominently in this slice. In addition, anatomical landmarks can be reliably used to identify this slice, thereby enabling the complete automation of this algorithm.

In this pilot study, manual segmentation by a physician expert is used as a gold standard ("ground truth") for validating the accuracy of the proposed method. Our aim was to develop an algorithm that could automate the process of 1) reliably finding the appropriate anatomic slice on a routine CT scan, and then 2) accurately segmenting the psoas muscle of interest.

2 RELATED WORKS

In addition to psoas muscles, there has been a growing interest in abdominal muscle segmentation, as a stratification tool in cancer treatment, pre-surgery treatment, surgical procedures and radiation. Early work done in this area used pre-defined Hounsfield Units (HU) to develop threshold based segmentation techniques. This approach can be reliably used to segment adipose tissue whose HU uniquely ranges from -190 to -30. However, muscle segmentation poses more challenges, since its HU values of -29 to 150, overlap with those of neighbouring organs.

Prior research in psoas muscle segmentation, primarily focuses on shape based models. Kamiya et al.(Kamiya et al., 2012) derived a mathematical function based shape model for segmenting the psoas muscle. However, this method still required the intervention of a radiologist in selecting the slice of interest. Meesters et al.(Meesters et al., 2012) presented an automatic system to assist the segmentation of abdominal organs, using the medially positioned psoas muscle's shape and location along with previously accomplished segmentation of the liver and spleen. However, owing to anatomical differences in patients, this method showed varying results. Gilles et al.(Gilles et al., 2006) introduced a modeling method for muscles in the crural area for analyzing their motor function in MR images. Ng et al.(Ng et al., 2007) introduced a recognition method, for surgical planning and analysis of loss of mastication function of the temporal muscle. These two methods, however, were used for MR images. The scalability of these methods to CT images still remains unclear since the boundaries between muscle and adjacent organs are not fundamentally different in such datasets.

Genetic Algorithms (GAs) have not been explored as a solution for psoas muscle segmentation. It proves to be a strong candidate if image segmentation is formulated as a numerical optimization problem. (Sheta et al., 2012) demonstrate how GAs complement existing optimization methods and has proved to be insensitive to noise. This characteristic proves extremely beneficial in medical imaging, in that GAs require no gradient information and hence they are less likely to get trapped in local minima on multimodal surfaces. Segmentation methods frequently use thresholds to decide whether two pixels are in the same region or not. However, the thresholds negatively affect the image segmentation and often result in inaccuracies. Therefore, the tuning values of the thresholding algorithms must be set up carefully (Levialdi et al., 2003; Hamdaoui et al., 2015). A multilevel thresholding method which allows the determination of the appropriate number of thresholds as well as the adequate threshold values has been proposed in (Hamdaoui et al., 2015). The paper combines both GA and wavelet transform. In this paper we propose a new method for image segmentation using GAs, by posing the segmentation problem as an optimization problem. The contribution of this work is the formulation of a set of tuning parameters for GAs to be effectively used on CT images. The authors have shown that GAs can be used as an intermediate step to develop an accurate segmentation map, which when combined with medical anatomical knowledge, produces accurate segmentation results for psoas muscle delineation. We will describe our works according to the following organization. The proposed model and the segmentation procedure are described in Section 3. The experimental results of the proposed model and some results compared with region growing models are shown in Section 4. At last, the conclusions are provided in Section 5.

3 PROPOSED METHOD

The proposed algorithm consists of two modules. The first module implements an automated identification of the L4 slice from the original CT images of the abdomen, which are provided as the module input. The slice containing the image of the L4 vertebra is determined. This is done by detecting the top of the iliac crest that acts as an anatomical landmark. The second module implements a GA based edge linking that identifies the pixels of the psoas muscle in the L4 slice

obtained from the first module.

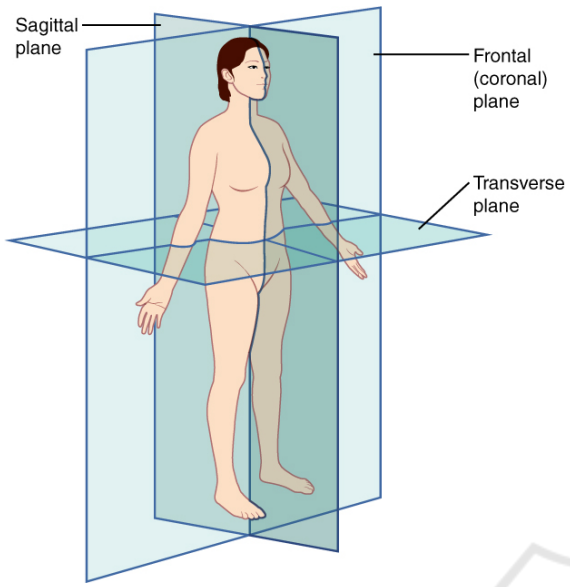

Figure 1: Planes of the Body.

3.1 L4 Identification

Before delving into the proposed method, it is important to understand terms used in the next sections, for describing anatomical landmarks. Fig. 1 (Jones, 2018) shows how a landmark can be represented in three dimensions. The terms superior and inferior are used for describing the position along the main body axis (representing top and bottom). Horizontally, the terms anterior and posterior are used for the front and back of the body respectively, while right and left is used for description of lateral points. Two-dimensional planes are used for describing cross-sections of the body. The sagittal plane is parallel to the body long axis and divides the body into left and right sections. The coronal plane is also parallel to the body axis and it divides the body to anterior and posterior sections. Finally, the axial plane, also known as transverse plane, is perpendicular to the body long axis and divides it to superior and inferior sections. The first module of our algorithm determines the L4 slice from the images of a CT scan. Medical literature highlights that the cross-section of the psoas muscle's transverse section is maximal at the longitudinal center and minimal at its origin and insertion. Parts of the skeletal muscles are connected to the skeleton. Hence, at the L4 vertebra, the radius of these muscles is likely the largest. Fig. 2 displays the flowchart of the L4 identification module. The identification method is mainly based on the anatomical location of the L4 vertebra.

In current clinical practice, radiologists commonly determine the L4 level in three steps (Farshad-Amacker et al., 2015): i) identifying the superior margin of the iliac crests in the coronal plane, followed by ii) connecting these points along the mediolateral axis, and then iii) selecting the vertebra superior to this axis. In our algorithm, this process is automated and streamlined by identifying the L4 level consistently at a level 2 cm above the iliac crests. Thus, we consider *'n'* slices as candidates to implement the algorithm to determine the L4 slice, where *'n'* depends on the separation of the slices in the series (for example, 5 mm or 2 mm or 1.25 mm, depending on the slice). For example, if the input images have a 5 mm separation, then we define the L4 level by selecting the image four slices above the top of the iliac crest. To do this manually over a large dataset proves to be extremely time consuming, and hence uneconomical.

The first author of this paper manually extracted the muscle regions. These regions were then inspected, and, if necessary, the results were revised by the third author, who is a medical expert on anatomy.

3.1.1 Pre-processing

In order to identify the iliac crests, the three-dimensional data was processed in the coronal plane. This required up-sampling followed by rotation while translating from axial to coronal plane. Fig. 3 shows the image of a slice from the coronal plane where the top of both the iliac crests are marked by red dots and the L4 vertebra is identified as 2 cm.

In order to optimize the algorithm we ran the next phase only on twenty slices. To determine these twenty slices, the contrast of all slices was enhanced by histogram equalization, after which the number of bone pixels in each slice were determined, based on a threshold. In order to determine this threshold, the image was first normalized after which it was fit to a normal distribution. A cumulative distributive function was used to determine the threshold, as the intensity value of the upper 90% of the pixels. Twenty

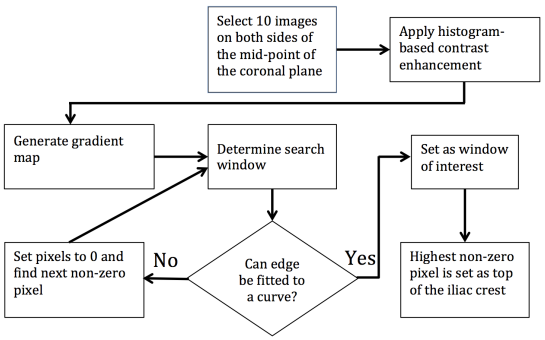

Figure 2: Flowchart of L4 Identification.

slices with the most number of bones pixels were chosen for the next step, in which the edge map was computed using a Canny edge detector. This step found edges by looking for local maxima in the image gradient (Canny, 1986). The gradient was then calculated using the derivative of a Gaussian filter. The method used two thresholds, to detect strong and weak edges, and included the weak edges in the output only if they are connected to strong edges. The algorithm was implemented in MATLAB and the default threshold values were chosen.

3.1.2 Search Window

Owing to the symmetric nature of the iliac crests, the recursive portion of the algorithm was run on each half of the image. The search window was initialized at the first pixel encountered on the edge map, towards the superior end of the image. The search window was then expanded with a maximum of 8x8 pixels, until the next pixel on the edge map was hit. This continued until the search window stopped growing in all directions. In a search window, if the non-zero pixel could be fitted to a curve, that was the window of interest containing the iliac crest. Otherwise, all pixels in that region were set to zero and the search window was initialized at the next non-zero pixel. In the search window of interest, the superior-most pixel on the edge map was the tip of the iliac crest. This L4 slice was determined at 2 cm above this point (taking into consideration the sampling performed during transformation between planes).

3.2 Proposed Genetic Algorithm (GA) based Edge Linking Method

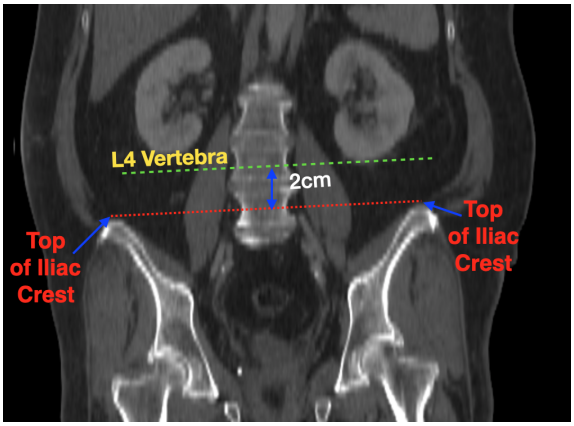

Figure 3: L4 Slice Detection.

In this paper, we propose a novel segmentation technique that has its foundation in GAs, to perform a semantic segmentation of the image. Fig. 4 highlights

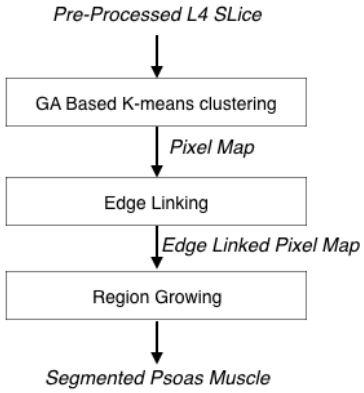

Figure 4: Overview of GA based Region Growing Method.

the main blocks of the proposed algorithm. At a high level, the GA is used to obtain a pixel map, where pixels are grouped by the likelihood that they belong to one class. The pixel map is then used, to perform a region growing in an edge linked constraint to obtain the final segmented image of the left and right psoas muscle. In the subsequent sections, we will go over details of each of these functional blocks. Before feeding the L4 slice into this part of the algorithm, the image is first pre-processed to highlight the bone and the areas surrounding it. This is done based on Otsu's thresholding.

3.2.1 Genetic Algorithm based K-means Clustering

Genetic algorithms have been proven to solve numerical optimization problems by stochastic search methods of the solution space. The premise of this algorithm is that a fitness function is used to obtain the best possible candidates for the final solution, in an iterative manner, through mutation, crossover and selection. GA's used earlier (Krishna and Murty, 1999) in clustering employ either an expensive crossover operator to generate valid child chromosomes from parent chromosomes or a costly fitness function or both. To circumvent these expensive operations, we hybridize GA with a classical gradient descent algorithm used in clustering like K-means algorithm. Hence, the name genetic K-means algorithm.

The GA consists of the following steps (Sheta et al., 2012):

1. Initialize population.
2. Compute fitness function at every pixel, based on fitness function.
3. Fittest individuals are selected for next iteration based on selection function.
4. Generate next population based on reproductive operators and fit members of current population.
5. Stop if stopping criterion is met, else go to step 3.

These steps are represented in Fig. 5.

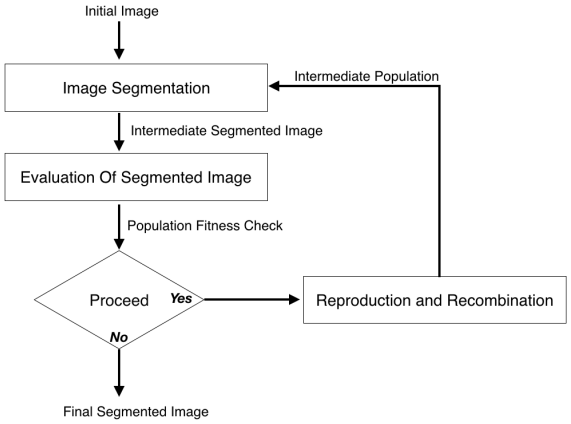

Figure 5: Segmentation using Genetic Algorithms.

Fitness Function:
In GAs, a fitness function is used to evaluate if individuals are capable of producing offsprings. In the proposed algorithm, a fitness function has been defined on the basis of the Euclidean distance computed between a given chromosome (i.e. pixel) and a region S. The fitness of an individual pixel, i is defined as follows

$$\Phi_i = min((G_k - i)^2) \quad (1)$$

where:
G_k, denotes the centroid of the kth cluster,
i, represents the pixel value at that location.

Selection Function:
The selection function used in the proposed algorithm is Roulette wheel, developed by Holland (Holland, 1992). The probability, P_i, for each individual is defined by:

$$P_i = \frac{F_i}{\sum_{j=1}^{PopulationSize} F_j} \quad (2)$$

where F_i, equals the fitness of individual i.
The use of roulette wheel selection limits the genetic algorithm to maximization since the evaluation function must map the solutions to a fully ordered set of values on fit. Extensions, such as windowing and scaling, have been proposed to allow for minimization and negativity.

Stopping Criteria:
The GA algorithm iterates through several generations until a stopping criteria is met. The proposed algorithm uses the specified number of maximum generations as its termination criterion.

3.2.2 Edge Linking and Region Growing

The technique of edge-based region growing (Singh et al., 2011) (Jamil et al., 2011) is chosen, as the left and right psoas muscles are in a contained region above the L4. As a first step, the edge map of the reduced region of interest is obtained by using canny edge operator. Edge linking is then performed by merging edges (Sappa and Vintimilla, 2008). Edge merging is done if the edge map contains discontinuities lesser than a given threshold, between pixels having similar gradient values. Fig. 6 shows the linked edges highlighted in red on the edge map.

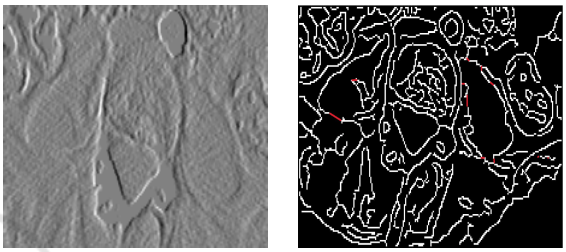

(a) Gradient Image (b) Highlighted Linked Edges

Figure 6: Edge Linking.

This makes the region growing much less noisy and is contained to the closed regions of the edges. Following the edge linking process, region growing is applied starting at the seed location determined in the previous section. The two parameters considered in the region growing process are: 1) the difference between a pixel's intensity value and the region's mean which is a measure of the similarity of the pixel to a given region and 2) if the pixel lies on the edge map. This process stops when the intensity difference between region mean and new pixel become larger than a certain threshold or if the pixel lies on the edge map. Region growing on the edge-linked edge map contains the region growing process to only the psoas muscle margin even if the difference in pixel intensity between the psoas and the surrounding abdominal muscles is not large.

4 RESULTS

We validated our algorithm on a dataset consisting of abdominal CT scans of 61 patients all over the age of 65 years with hip fractures (32 female and 29 male).

The CT scans on average have 90 images in every series. These images are 512x512, with a bit depth of 16 bits captured via helical scan mode. 90% of these images do not have any contrast agent. The presence of a contrast agent is seen to boost the accuracy of

the algorithm. In this cohort all the scans have a slice thickness of 5mm. The algorithm performs well at this value. However, for some, 1.25mm slice thickness were also available. The algorithm did not show promising results at this thickness owing to the high amount of noise in these images.

Table 1: Results of L4 Identification.

	Range of L4 Slices (ground truth)	L4 Slice (proposed method)
patient1	27-32	31
patient2	51-56	51
patient3	2-7	4
patient4	41-46	42
patient5	33-37	36
patient6	44-49	49
patient7	42-47	44
patient8	39-44	43
patient9	37-42	50

To evaluate the accuracy of the L4 identification, a radiologist was asked to identify the range of L4 slices in each dataset. The accuracy of this module is determined by the number of slices by which the algorithm misses the required L4 range, as manually determined by a domain expert (radiologist). Table 1 shows a sampling of the results for the L4 identification module of the algorithm. The datasets were chosen such that each has a unique position for the L4 slice. This ensures the robustness of the algorithm. Even when the iliac crests were not exactly symmetric, the algorithm performed accurately across such datasets. As can be seen in Table 1, our algorithm failed to correctly identify the position of L4 slice of patient9 and obtained a difference of 8 slices relative to the ground truth. This was the case where the algorithm performed the worst. On retrospective analysis, we found out that this dataset did not have sufficient contrast difference between the psoas and the surrounding abdominal soft tissues. Out of the 61 CT images, about 12 datasets missed the L4 window with an error of 1-8 slices. This will be addressed in future research, by incorporating the shape model of the psoas muscle to improve the accuracy of the algorithm. The initial population of the Genetic Algorithm was randomly selected. The population size of 50 was chosen. A stopping factor of 100 generations was selected for these runs. Fig.7 shows that, for a CT image at the L4 slice, the fitness function converges within the selected stopping criteria of 100 generations. At the end of this stage, the GA driving k-means segmentation generates a segmentation map as shown in Fig.8 and Fig.9. Note, Fig.8, shows the

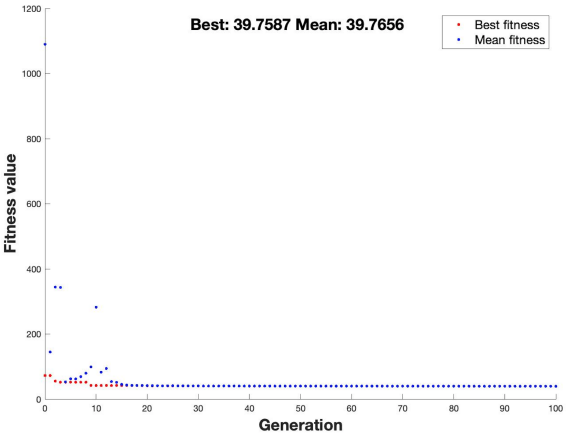

Figure 7: Convergence of Genetic Algorithm.

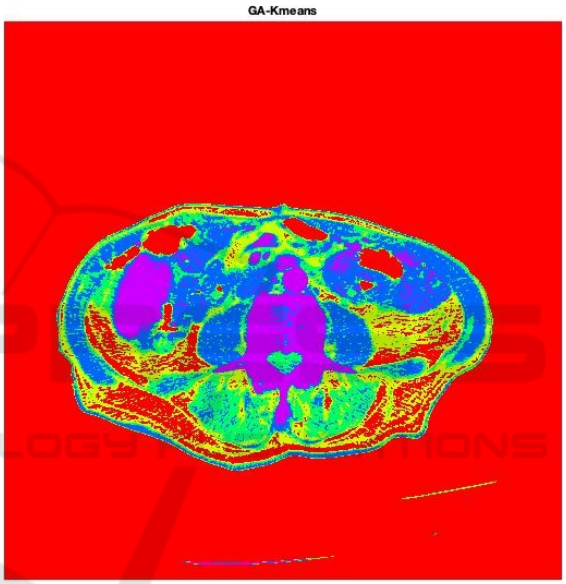

Figure 8: Segmentation map produced by Genetic Algorithm.

various classes highlighted in HSV color space. This is done for the sake of representation only. The proposed method consumes a gray scale version of this, as represented in Fig 9. For evaluating the accuracy of the psoas muscle segmentation algorithm, we compared the manual segmentation as performed by a radiologist and our semi-automatic segmentation algorithm of the abdominal CT scans. The results of two datasets are shown in figures 10 and 11.

In order to quantify our results, we have computed the true positive percentage as the number of pixels labelled as psoas in both the ground truth and the output of our algorithm. False positives are pixels marked as psoas by our algorithm and not psoas in the ground truth. Finally, we have false negatives as pixels that are actual psoas muscle pixels in the ground truth, and that are not labeled by our algorithm.

Figure 9: Segmentation map produced by Genetic Algorithm.

Table 2: Results of Psoas Segmentation.

	True positive rate (%)	False positive rate (%)	False negative rate (%)
patient1	86.47	7.64	25.87
patient2	87.33	16.70	15.96
patient3	91.59	5.11	3.28
patient4	84.25	7.44	8.30
patient5	89.62	1.88	8.49
patient6	92.76	1.82	14.41
patient7	83.64	13.42	2.92
patient8	83.10	3.11	13.79
patient9	95.10	1.72	19.18

These results that are computed across the dataset are tabulated in Table 2. Our algorithm showed relatively low detection rates on three datasets, i.e. patient 1, 2 and 9. Because these three datasets of lower contrast, result in the details around edges be lost. In particular, our algorithm failed to identify the correct position of L4 slice for patient9. The dataset corresponding to patient9 showed lower true positive percentage, as it failed to correctly identify the correct L4 slice.

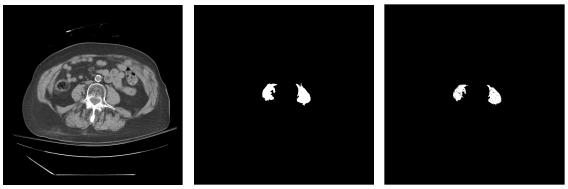

(a) L4 Slice (b) Ground Truth (c) Our Result

Figure 10: Psoas Segmentation Results.

(a) L4 Slice (b) Ground Truth (c) Our Result

Figure 11: Psoas Segmentation Results.

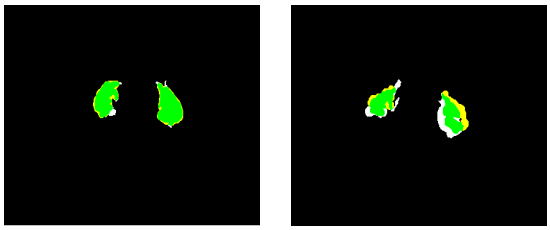

(a) patient2 (b) patient1

Figure 12: Accuracy of Psoas Segmentation Algorithm.

In Fig. 12(a) and (b) we use the detected results of patients1 and patient2, respectively, to show how the numbers in Table 2 are calculated. The true positives (TP) are highlighted in green, false negatives (FN) are highlighted in white and false positives (FP) are shown in yellow.

5 CONCLUSION

We present a semi-automatic method to identify images corresponding to the 4^{th} lumbar vertebra and then identify the left and right psoas muscles in this slice. Anatomical landmarks were set up in a completely automatic manner with the use of spatial positioning information on the images. The algorithm was tested on 61 datasets. The L4 identification module of the algorithm shows accurate results in about 80% of the cases. The failing cases were primarily scans with poor resolution and contrast, which resulted in irregularities of muscle boundaries. This proved to be a breaking point of this algorithm, that relied on edge linking.

The psoas muscle segmentation module recorded average true positive rate of 91%. As next steps, the accuracy of the algorithm will be enhanced by improving the accuracy of the edge linking phase of the segmentation algorithm. This will in turn preserve details around edges of the psoas muscle. Our approach met the criterion laid out by radiologists to replace the current manual process of psoas muscle identification around the L4.

ACKNOWLEDGEMENTS

The research in this paper was partially supported by National Institutes of Health under award number R01 AR076088. The authors would like to thank Dr. Stephen Henrichon of the University of California, Davis, who provided access to scans as well as training on image interpretation.

REFERENCES

Alfonso J. Cruz-Jentoft, Jean Pierre Baeyens, e. a. (2019). Clinical definition of sarcopenia. *Sarcopenia: European consensus on definition and diagnosis: Report of the European Working Group on Sarcopenia in Older People, Age and Ageing*, 39(4):412–423.

Canny, J. (1986). A computational approach to edge detection. *Pattern Analysis and Machine Intelligence, IEEE Transactions on*, PAMI-8(6):679–698.

Cornet, M., Lim, C., Salloum, C., Lazzati, A., Compagnon, P., Pascal, G., and Azoulay, D. (2015). Prognostic value of sarcopenia in liver surgery. *Journal of visceral surgery*, 152(5):297-304.

Farshad-Amacker, N. A., Aichmair, A., Herzog, R. J., and Farshad, M. (2015). Merits of different anatomical landmarks for correct numbering of the lumbar vertebrae in lumbosacral transitional anomalies. *European Spine Journal*, 24(3):600–608.

Gilles, B., Moccozet, L., and Magnenat-Thalmann, N. (2006). Anatomical Modelling of the Musculoskeletal System from MRI. *Medical Image Computing and Computer-Assisted Intervention – MICCAI 2006*, 4190:289–296.

Hamdaoui, F., Sakly, A., and Mtibaa, A. (2015). An efficient multi level thresholding method for image segmentation based on the hybridization of modified pso and otsu's method. *Computational Intelligence Applications in Modeling and Control*, 2003:343–367.

Holland, J. H. (1992). *Adaptation in Natural and Artificial Systems: An Introductory Analysis with Applications to Biology, Control and Artificial Intelligence*. MIT Press, Cambridge, MA, USA.

Jamil, N., Soh, H., Tengku Sembok, T., and Bakar, Z. (2011). A Modified Edge-Based Region Growing Segmentation of Geometric Objects. *Visual Informatics: Sustaining Research and Innovations*, 7066(4):99–112.

Jones, O. (2018). Anatomical Planes.

Kamiya, N., Zhou, X., Chen, H., Muramatsu, C., Hara, T., Yokoyama, R., Kanematsu, M., Hoshi, H., and Fujita, H. (2012). Automated segmentation of psoas major muscle in X-ray CT Images by use of a shape model: preliminary study. *Radiological Physics and Technology*, 5(1):5–14.

Krishna, K. and Murty, M. (1999). Genetic k-means algorithm. *IEEE transactions on systems, man, and cybernetics. Part B, Cybernetics: A publication of the IEEE Systems, Man, and Cybernetics Society*, 29:433–9.

Levialdi, S., Cinque, L., Cucchiara, R., and Pignalberi, G. (2003). Tuning range image segmentation by genetic algorithm. *EURASIP Journal on Advances in Signal Processing*, 2003.

Meesters, S., Yokota, F., Okada, T., Takaya, M., Tomiyama, N., Yao, J. J., Liguraru, M., Summers, R., and Sato, Y. (2012). Multi atlas-based muscle segmentation in abdominal CT images with varying field of view. *Med Image Anal.*

Ng, H., Hu, Q., Ong, S., Foong, K., Goh, P., Liu, J., and Nowinski, W. (2007). Segmentation of the temporalis muscle from MR data. *International Journal of Computer Assisted Radiology and Surgery*, 2(1):19–30.

Santilli, V., Bernetti, A., Mangone, M., and Paoloni, M. (2014). Clinical definition of sarcopenia. *Clinical cases in mineral and bone metabolism: the official journal of the Italian Society of Osteoporosis, Mineral Metabolism, and Skeletal Diseases*, 11(3):177-180.

Sappa, Angel, D. and Vintimilla, Boris, X. (2008). Edge Point Linking by Means of Global and Local Schemes. *Signal Processing for Image Enhancement and Multimedia Processing*, 31(4):115–125.

Sheta, A., Braik, M. S., and Aljahdali, S. (2012). Genetic algorithms: A tool for image segmentation. In *2012 International Conference on Multimedia Computing and Systems*, pages 84–90.

Singh, R., Singh, J., Sharma, P., and Sharma, S. (2011). Edge based region growing. *International Journal of Computer Technology and Applications*, 2(4).

Ulf Tiede, Thomas Schiemann, K. H. (1996). Visualizing the Visible Human. *IEEE Computer Graphics and Applications*, 16(1):7–9.

Van Ancum, J. M. (2020). Impact of using the updated ewgsop2 definition in diagnosing sarcopenia: A clinical perspective. *Archives of gerontology and geriatrics*.